Laboratory and numerical studies of solitary and N-waves

Lima, V. (1, 2, 4); Avilez-Valente, P. (3,4); Baptista, M. A. (2,5); Miranda, J. M. (2,6)

(1) Instituto Hidrográfico (IH), vania.lima@hidrografico.pt.

(2) Instituto Dom Luiz, FCUL (IDL).

(3) Faculdade de Engenharia da Universidade do Porto (FEUP).

(4) Centro Interdisciplinar de Investigação Marinha e Ambiental, UP (CIIMAR).

(5) Instituto Superior de Engenharia de Lisboa (ISEL).

(6) Instituto Português do Mar e da Atmosfera (IPMA).

Abstract: When no field data is available or a conceptual analysis is envisaged, it is a common approach to model tsunamis as solitary waves (SW), both in experimental and numerical studies. However, it has been suggested that N-shaped waves are more adequate to describe the main tsunami wave.
The usual method for laboratory generation of SW is based on the first-order wave-maker theory, for a piston-type wave-maker. For the laboratory generation of N-waves (NW), using a piston-type wave-maker, a novel first-order formulation was introduced.
Laboratory experiments for 76 wave cases of propagation of S- and N-waves were performed at the Laboratory of Hydraulics (LH) of the Faculty of Engineering of the University of Porto. Laboratory measurements of S- and leading depression N-waves are analysed and compared to numerical simulation results obtained with OpenFOAM. Improvements and future work are suggested.

Key words: N-wave, OpenFOAM, piston-type wave-maker, solitary wave, tsunami modelling.

1. INTRODUCTION

The most used method for the generation of solitary waves (SW) in a laboratory is based on the first order wave-maker theory of Goring (1978) and Goring and Raichlen (1980) for a piston type wave-maker. Goring's procedure, which is based on the Boussinesq first-order solitary wave solution, is a method limited to waves with a small height-to-depth ratio. A detailed literature review showed vast research work concerning the generation of solitary waves (Lima *et al.*, 2019). However, it revealed a considerable lack of work on the process of N-wave (NW) generation in a wave flume, by means of a piston wave-maker. In Lima *et al.* (2019), the authors propose a novel formulation for the generation of N-waves with piston wave-makers, by extending Goring's method (Goring, 1978; Goring and Raichlen, 1980) for the Boussinesq solitary wave to the general N-wave expression introduced by Tadepalli and Synolakis (1994, 1996a).

Using Goring's formulation for the laboratory generation of solitary waves with piston wave-makers and the novel first-order formulation for the generation of N-waves with piston wave-makers (introduced by Lima *et al*. 2019), new laboratory experiments were conducted. Here, 76 wave cases of SW and NW were generated along a channel with constant section, with and without a beach assembled, and their propagation was recorded. Laboratory measurements of some of the wave cases performed were analysed and compared with the expected theoretical profiles and with the numerical simulations' results obtained with OpenFOAM (OpenCFD Limited, 2019), specifically with the olaFlow package (Higuera, 2019).

2. DESCRIPTION OF THE EXPERIMENTS

2.1 Wave basin physical experiments

For the wave basin physical experiments (Figure 1) with constant water depths d of 25 and 50 cm, 16 paddles of the wave generation system were activated.

Fig. 1. Wave basin at the LH, FEUP. Setting of the wave gauges used in the basin experiments.

A set of 4 wave gauges were installed on tripods and fixed on the basin floor. We placed 3 wave gauges 1.30 m away from the wave-maker, 5.25 m apart from each other (Figure 2). For control purposes, wave gauge wg6 was placed behind wg1/wg5, distanced 1.20 m. The time series measurements were acquired and recorded by the HR Wallingford (HRW) software program (HRW DAQ Suite version 1.24.0.0).

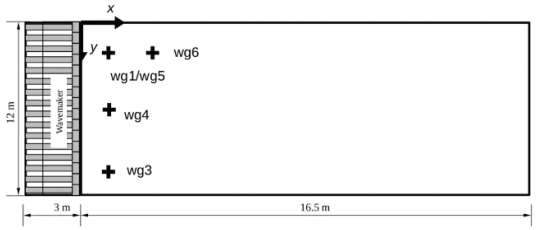

Fig. 2. Wave basin and wave gauges' positioning used for the constant water depths (25 and 50 cm) experiments

2.2 Plane slope physical experiments (with beach)

A channel with 1.5 m width was constructed inside the wave basin, limited on one side by a Perspex wall along the tank and by its side wall. A beach composed by two slopes with 1:15 and 1:30 respectively was assembled along the channel (Figure 3). This beach is composed by one flat 5 m long section starting right after the wave-maker, followed by a 1:15 plane slope (angle β1) with 3.75 m of length and a second plane slope (angle β2) with 7.5 m of length and 1:30. Only 2 wave-maker paddles were activated for the experiments inside the channel, as the limiting plexiglass wall was extended up to the paddles.

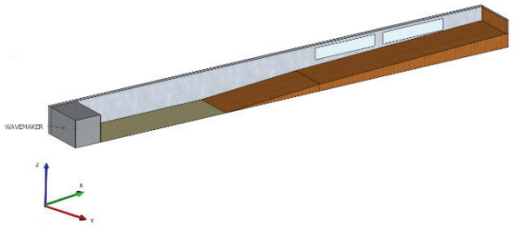

Fig. 3. Scheme of the beach profile assembled inside the wave basin, in a 1.5 m wide channel, composed by a flat 5 m section and 2 slopes with 1:15 and 1:30, respectively.

The experiments were performed for two levels of water depth: 25 cm and 50 cm (Figures 4, 5 and 6).

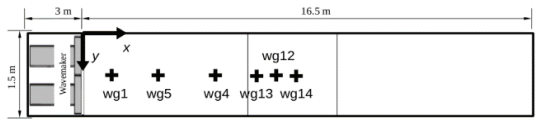

Fig. 4. Wave gauges' positioning inside the 1.5 m wide channel, for the 25 cm water depth experiments.

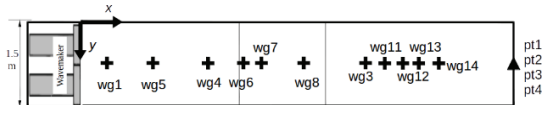

Fig. 5. Wave gauges' positioning inside the 1.5 m wide channel, for the 50 cm water depth experiments.

For the experiments with the beach, a maximum of eight long wave gauges were installed on fixed arms, mounted on the side wall of the wave basin, and three short wave gauges were installed on small tripods, to measure data in reduced water depth (Figures 4 to 6).

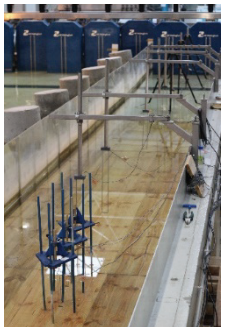

Fig. 6. Wave gauges setting along the channel, for 50 cm water depth experiments.

2.3 Wave conditions

We defined a set of solitary waves (SW) and N-waves (NW) to be generated (Table 4.9 in Lima, 2020) with wave heights between 6 and 24 cm, for water depths of 25 cm and 50 cm and for piston strokes between 0.25 m and 1.00 m.

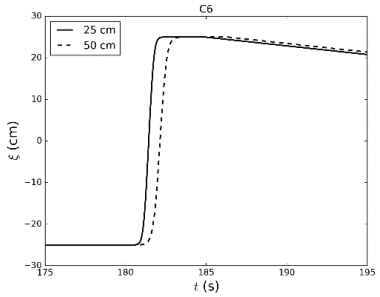

Fig. 7. Piston trajectory for the generation of solitary wave C6, with 50 cm stroke, for water depths of 25 (C6a) and 50 cm (C6b).

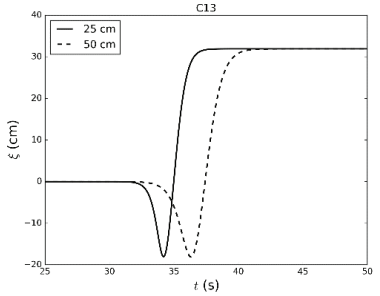

Fig. 8. Piston trajectory for the generation of LDN-wave C13, with 50 cm stroke, for water depths of 25 (C13a) and 50 cm (C13b).

The solitary waves generated were positive shaped. The N-waves generated were leading depression (LDN) type, with ratio a– / a+ = 0.4, which means that H = 1.4 × a+. This ratio was found to present the best fitting results both in the preliminary experimental and numerical tests (Lima, 2020). The piston wave-maker trajectories for waves C6 (H = 0.155 m) and C13 (H = 0.085 m) are represented in Figures 7 and 8 respectively.

3. NUMERICAL SIMULATIONS

The computational simulations were performed using OpenFOAM and the olaFlow toolbox. The

computational domain for the olaFlow numerical tests is a replication of the wave channel. A 2DV model is used and the computational domain is set into 3 blocks specified inside blockMeshDict. The number of cells in the *x* direction is 200 and 50 in the *z* direction. The boundary condition applied uses the wave type wave-maker with the wavemakerMovementDict dictionary. For that purpose, a text file was created beforehand and used for the simulations. The text file is composed by a time series with the data for the several paddle positions and the free surface elevation at each paddle position.

In terms of turbulence modeling, the olaFlow's library with the modified κ – ε and κ – ω turbulence models enables the code to more accurately simulate multiphase systems. Devolder *et al.* (2017) explained that κ – ε and κ – ω turbulence models caused more wave damping over the wave flume's length and therefore implemented a modified turbulence model, the κ – ω SST model. This was the turbulence model selected to use in the numerical simulations, as the modified turbulence model κ – ω SST prevents significant wave damping over the length of the wave flume (Devolder *et al.*, 2017).

4. RESULTS AND DISCUSSION

We consider the solitary waves (SW) and leading depression N-waves (LDN) experiments performed in the LH-FEUP wave tank (Figures 1 and 2), with the physical model of a beach composed by two slopes 1:15 and 1:30 (Figure 3 to 6), for 2 water levels of 25 and 50 cm water depths.

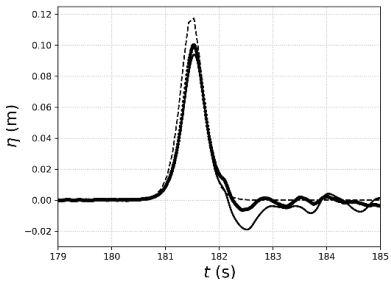

Fig. 9. Comparing results at wg1/wg5 for experimental SW C203a (stroke 50 cm), for wave basin experiments (—), with beach (**) and analytical TS (--) (25 cm water depth).

For the experiments within the tank (Figure 2), comparison for the same wave gauge is presented for C203 and C303 (solitary and N-wave with H = 12 cm respectively and stroke 50 cm) in Figures 9 and 10, for a water depth of 25 cm (C203a and C303a), and in Figures 11 and 12 (C203d and C303d), for a water depth of 50 cm. The theoretical time series (TS) is also plotted. It was found that there is a more pronounced difference in the comparison plot for the SW at 50 cm water depth. Noise at wg5 was predominant in these measurements, with a distinct shift between wave profiles (Figures 11 and 12).

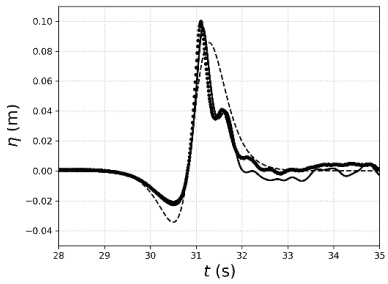

Fig. 10. Comparing results at wg1/wg5 for experimental NW C303a (stroke 50 cm), for wave basin experiments (—), with beach (**) and analytical TS (--) (25 cm water depth).

The Stokes number St for each wave case experimented (Table 4.9 in Lima, 2020) was determined. The expression for the Stokes number is:

$$St = \epsilon / \sigma^2 .$$

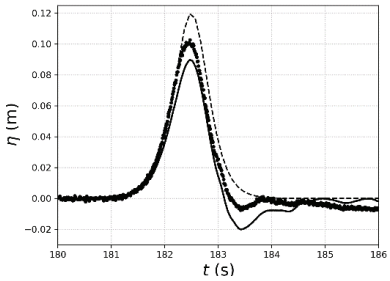

Fig. 11. Comparing results at wg1/wg5 for experimental SW C203d (stroke 50 cm), for wave basin experiments (—), with beach (**) and analytical TS (--) (50 cm water depth).

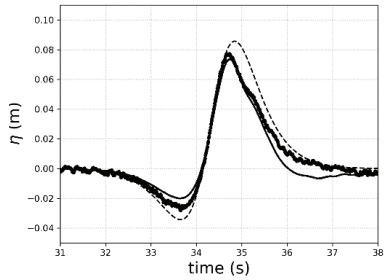

Fig. 12. Comparing results at wg1/wg5 for experimental NW C303d (stroke 50 cm), for wave basin experiments (—), with beach (**) and analytical TS (--) (50 cm water depth).

The Stokes number St relates the waves' non-linearity and dispersion and classifies the wave cases according to their characteristics and behaviour. The limits on this classification scale are flexible and we defined three increasing intervals for St : St < 3 correspond to short Boussinesq waves; 3 < St < 10 correspond to a mixed behaviour, and St > 10 correspond to long non-Boussinesq waves (Lima *et al.*, 2019). Most of the waves experimented, SW and LDN, have mixed behaviour; a part of the SW show a behaviour closer to short Boussinesq waves and part of the NW show long non-Boussinesq waves behaviour.

The comparison between the experimental and numerical SW propagation for C6a, with H = 15.5 cm, 50 cm stroke and d = 25 cm (Lima, 2020), shows that, although the numerical wave height is 25% less

than the laboratory measurement, the shape is similar to what was obtained experimentally. The wave displays a step-like shape and becomes unstable as the slope starts. Experimentally, a series of smaller waves are observed before the generated solitary wave, which are most probably a consequence of lateral wall reflections. For C13a, with H = 8.5 cm, 50 cm stroke and d = 25 cm (Lima, 2020), it is observed in the first wave gauge register that the N-wave crest is already in fission and its trough is larger than expected. The fission originates the division of the wave crest in two and in the following wave gauges several trailing waves are observed, as well as an increase of the crest's wave height.

For the 50 cm water depth experiments, the SW C6b, with H = 15.5 cm, 50 cm stroke and d = 50 cm (Lima, 2020), numerical wave height is 15% less than the laboratory measurement but the wave shapes are similar. There is a larger trough following the solitary wave. At the wave gauge located in the middle of the second slope–although following what is observed from the experiments–, the wave starts to rumble losing its shape. Afterwards, the wave crest assumes a step-like shape. Comparing the 50 cm N-wave physical experiments (H = 8.5 cm and 50 cm stroke) with the numerical simulations, is observed that the N-wave generated with the numerical wave-maker is closer to the input theoretical LDN-wave. At an early stage, the wave trough starts displaying several smaller waves, with increase of the wave crest tending to a solitary wave shape. As the experimental wave progressively decreases in height, in the numerical simulation the wave is continuously increasing. This could be related to the fact that bottom friction was not contemplated in the numerical simulation.

5. CONCLUSIONS

Laboratory experiments of solitary and LDN-waves on the wave basin and on a beach with two different slopes have been described. Measurements of the water surface elevation were retrieved from the physical experiments. The waves generated were characterizes according to their Stokes number. We found that for both solitary and LDN-waves the measured wave height H is systematically less than what was initially expected, when comparing with the theory and with the numerical simulations using the theoretical wave profile as input. The wave celerity formulations adopted for the solitary and N-waves seem to be adequate, when comparing measurements and simulations with olaFlow.

The comparison between the experimental and the simulations' results show overall good agreement for both the solitary and N-waves studied, although there is an underestimation of the numerical wave height. As future work, it is proposed to perform numerical tests with time-dependent wave celerity formulations, as it might lead to an increased accuracy in the obtained N-wave profile.

Acknowledgements

First author was supported by FCT grant SFRH/BD/96725/2013. Research partially supported by the Research Line ECOSERVICES, integrated in the Structured Program of R&D&IINNOVMAR: Innovation and Sustainability in the Management and Exploitation of Marine Resources (NORTE-01-0145-FEDER-000035), funded by the Northern Regional Operational Programme (NORTE 2020) through the European Regional Development Fund.

REFERENCES

Devolder B., Rauwoens P. and Troch P. (2017). Application of a buoyancy-modified κ – ω SST turbulence model to simulate wave run-up around a monopile subjected to regular waves using OpenFOAM®. *Coastal Engineering*, 125, 81–94.

Goring D. (1978). *Tsunamis – The Propagation of Long Waves onto a Shelf*. PhD Thesis, W.M. Keck Laboratory of Hydraulics and Water Resources, California Institute of Technology.

Goring D. and Raichlen F. (1980). The generation of long waves in the laboratory. In *Proceedings of 17th Conference on Coastal Engineering*, Sydney, Australia, 1980 (Edge B.L., ed.), 763–783. ASCE.

Higuera P. (2019). *olaflow*. https://olaflow.github.io/,

https://doi.org/10.5281/zenodo.1297012. Accessed: 2019-04-29.

Lima, V. V., Avilez-Valente, P., Baptista, M.A. and Miranda, J.M. (2019). Generation of N-waves in laboratory. *Coastal Engineering*, 148, 1-18.

Lima, V. V. (2020). *A Combined Model for Tsunami Wave Propagation, Dispersion, Breaking and Fluid-Structure Interaction.* (Unpublished doctoral dissertation). FCUL, Portugal.

OpenCFD Limited (2019). *OpenFOAM® - The Open Source CFD Toolbox*. https://www.openfoam.com/. Accessed: 2019-01-22.

Tadepalli S. and Synolakis C. (1994). The run-up of N-waves on sloping beaches. *Proceedings of the Royal Society London: Mathematical and Physical Sciences*, A445:99–112.

Tadepalli, S., Synolakis, C.E. (1996). Model for the leading waves of tsunamis. *Phys. Rev. Lett.* 77, 2141–2144.